

Supporting Information

Polarity and Moisture Induced Trans-grain-boundaries 2D/3D Coupling Structure for Flexible Perovskite Solar Cells with High Mechanical Reliability and Efficiency

Ying Yan,^{*a} Ruiting Wang,^{a,b} Qingshun Dong,^{*b} Yanfeng Yin,^c Linghui Zhang,^d Zhenhuang Su,^e Chenyue Wang,^e Jiangshan Feng,^f Minhuan Wang,^d Jing Liu,^d Hongru Ma,^b Yulin Feng,^d Wenzhe Shang,^b Zhiyong Wang,^{a,b} Mingzhu Pei,^b Yudi Wang,^b Shengye Jin,^c Jiming Bian,^d Xingyu Gao,^e Shengzhong Liu,^{f,g} Yantao Shi^{*b}

- a. Key Laboratory for Precision and Non-traditional Machining Technology of Ministry of Education, Dalian University of Technology, Dalian 116024, China
Email: yanying@dlut.edu.cn
- b. State Key Laboratory of Fine Chemicals, Frontier Science Center for Smart Materials, Department of Chemistry, School of Chemical Engineering, Dalian University of Technology, Dalian 116024, China
Email: dongqs@dlut.edu.cn, shiyantao@dlut.edu.cn
- c. State Key Laboratory of Molecular Reaction Dynamics, Dalian Institute of Chemical Physics, Chinese Academy of Sciences, Dalian 116023, China
- d. Key Laboratory of Materials Modification by Laser, Ion, and Electron Beams (Ministry of Education), School of Physics, Dalian University of Technology, Dalian 116024, China
- e. Shanghai Synchrotron Radiation Facility, Shanghai Advanced Research Institute, Shanghai Institute of Applied Physics, Chinese Academy of Sciences, Shanghai 201204, China
- f. Key Laboratory of Applied Surface and Colloid Chemistry, Ministry of Education, Shaanxi Key Laboratory for Advanced Energy Devices, Shaanxi Engineering Lab for Advanced Energy Technology, School of Materials Science and Engineering, Shaanxi Normal University, Xi'an 710119, China
- g. Dalian National Laboratory for Clean Energy, iChEM, Dalian Institute of Chemical Physics, Chinese Academy of Sciences, Dalian 116023, China

* Corresponding author

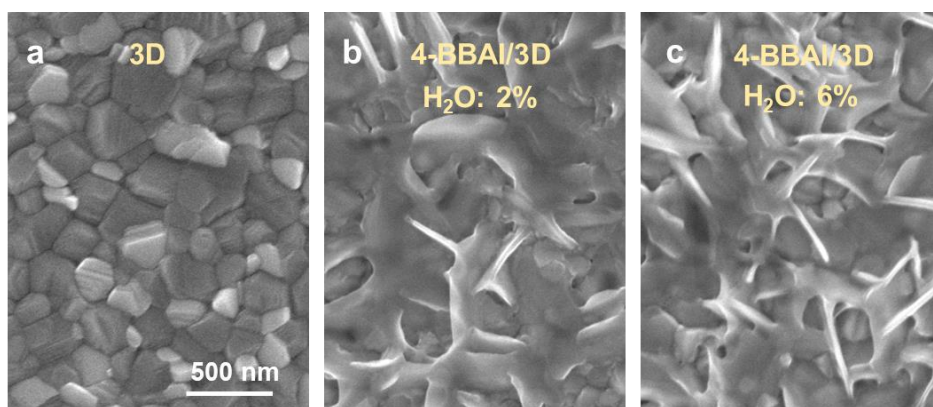


Fig. S1 Top-view SEM images of the 3D MHP thin film **(a)**, and that after deposition with 4-BBAI inside the glove box, where the solvent (IPA) of the 4-BBAI solution contains 2% H₂O **(b)** and 6% H₂O **(c)**.

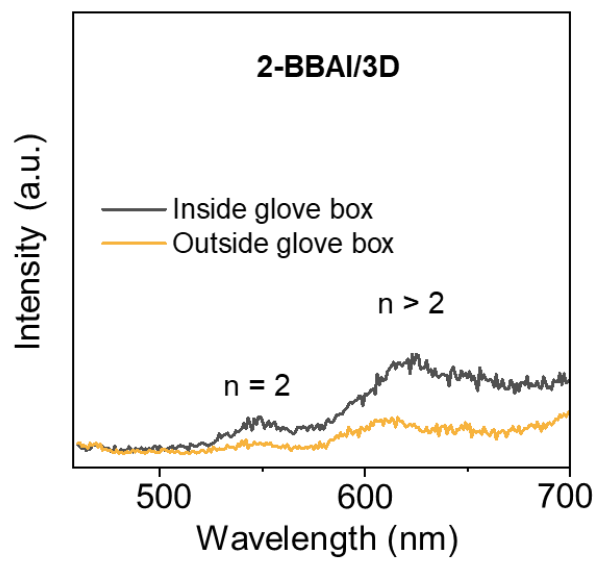


Fig. S2 PL spectra (zoom in on the y-axis) of the 2-BBAI/3D MHP thin films, where the 2-BBAI was deposited inside or outside the glove box.

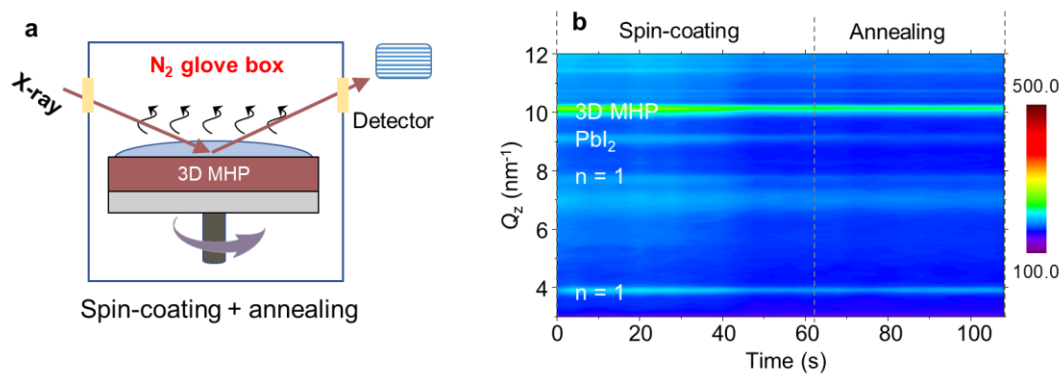


Fig. S3 (a) Schematic of in situ GIWAXS characterization illustrating deposition of 2D MHP on 3D MHP by spin-coating and annealing process in the N₂ glove box. (b) 2D intensity-time color mappings during 4BBAI-based 2D MHP deposition process in the N₂ glove box.

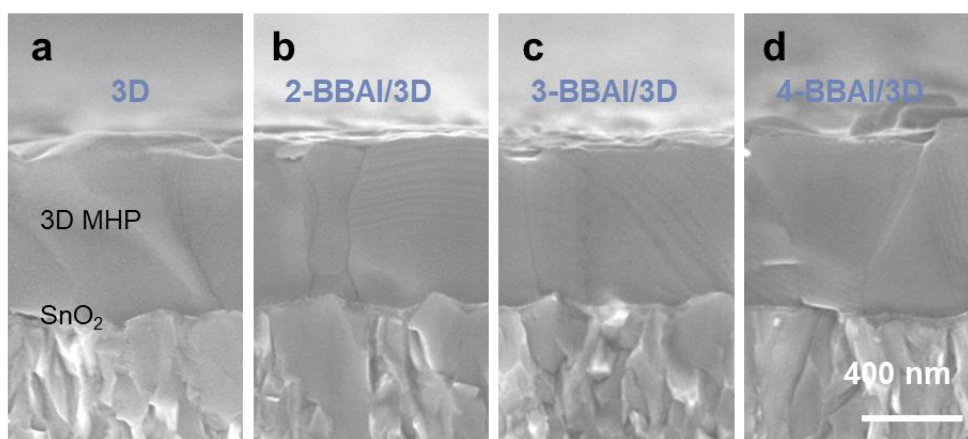


Fig. S4 Cross-sectional SEM images of the 3D MHP thin film with large grain size **(a)**, and that after deposition with 2-BBAI **(b)**, 3-BBAI **(c)**, and 4-BBAI **(d)** under ambient conditions.

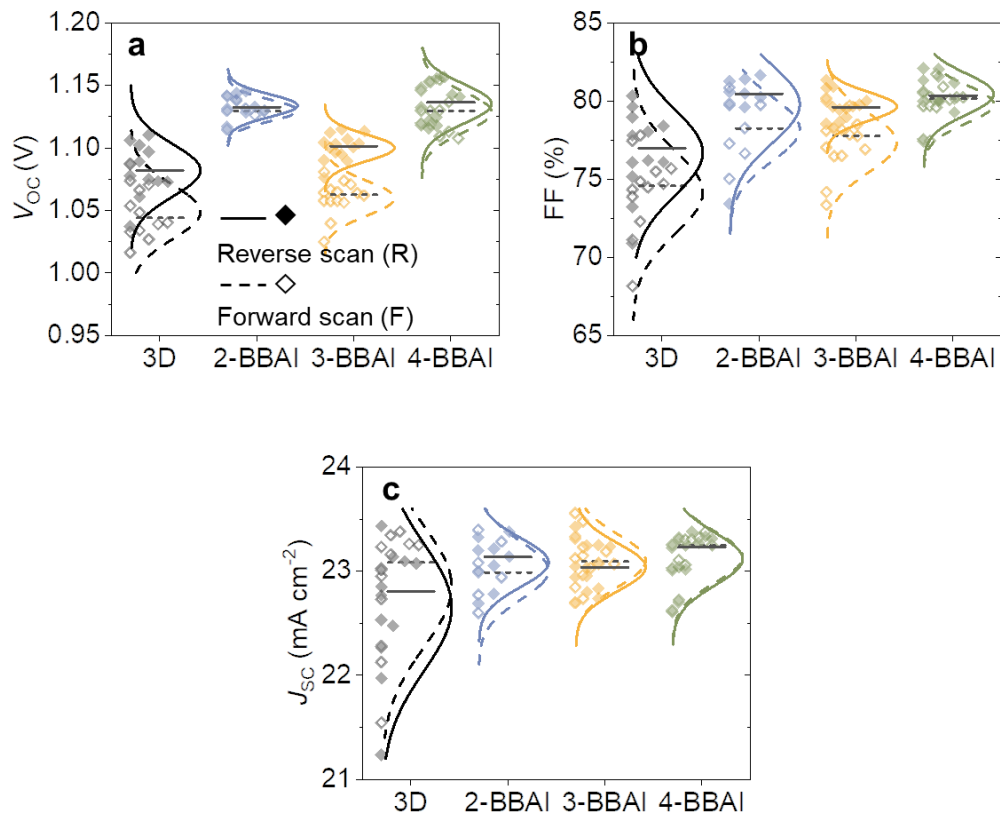


Fig. S5 The distribution of PV performance parameters (in reverse and forward scans) of f-PSCs with and without the 2D MHP capping layer: **(a)** V_{oc} , **(b)** FF, and **(c)** J_{sc} .

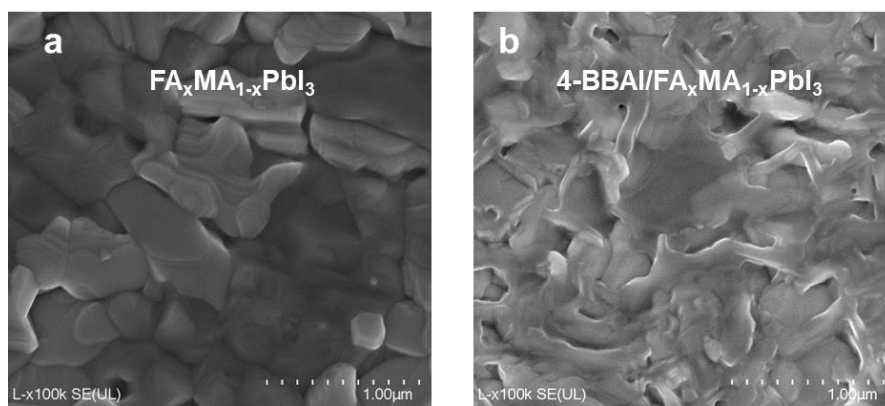


Fig. S6 Top-view SEM images of the “two-step” method deposited FA_xMA_{1-x}PbI₃ MHP **(a)**, and that after deposition with 4-BBAI solution outside the glove box **(b)**.

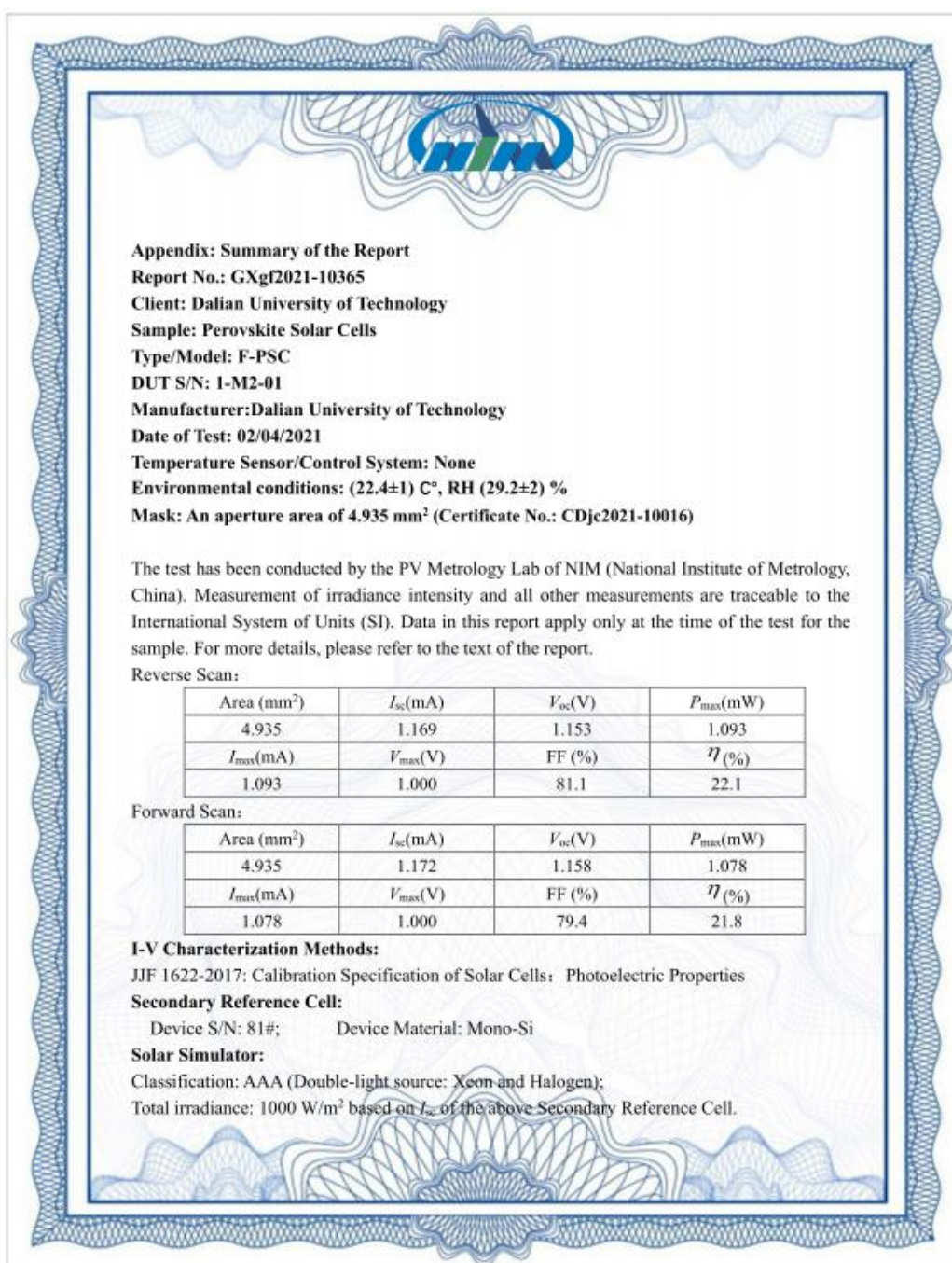


Fig. S7 Certificated PV performance from National Institute of Metrology, China. The certificated efficiency is 22.1% (reverse scan) and 21.8% (forward scan) for the best f-PSC based on 4-BBAI/ FA_xMA_{1-x}PbI₃ 2D/3D MHP.

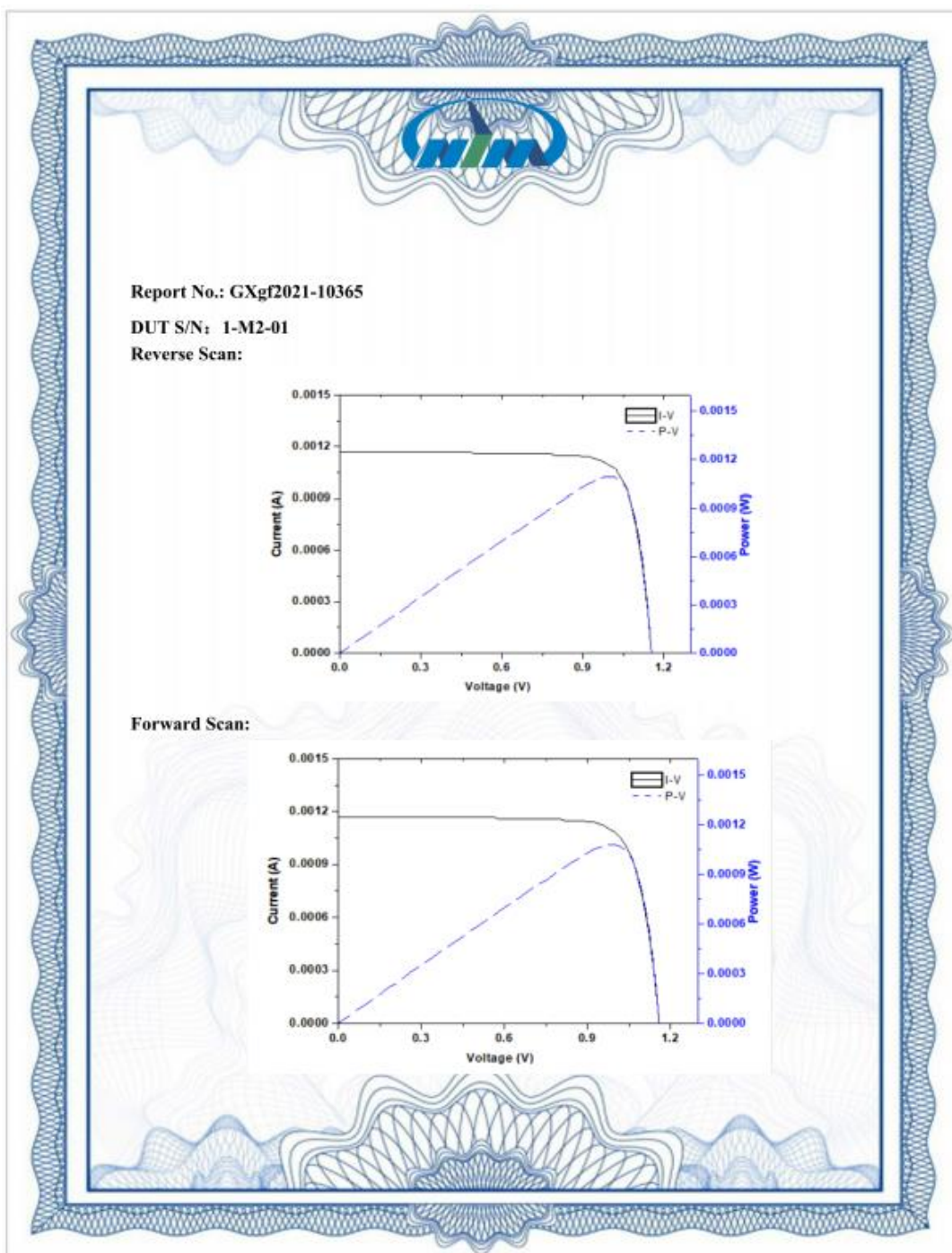


Fig. S8 *I-V* curves for the best f-PSC based on 4-BBAI/ FA_xMA_{1-x}PbI₃ 2D/3D MHP.

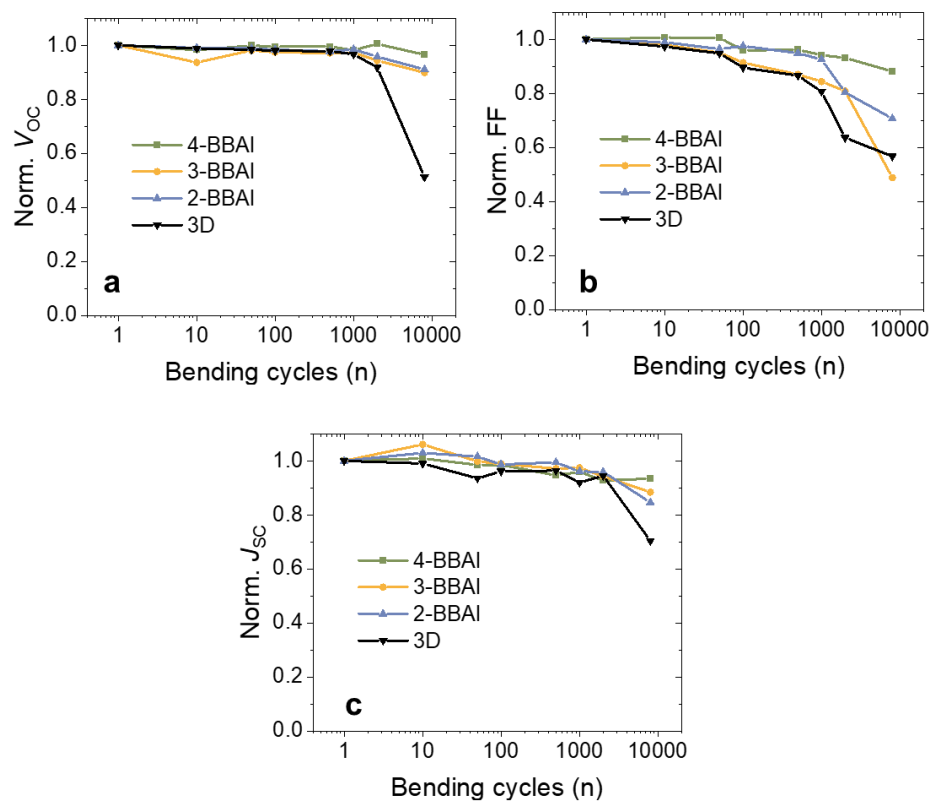


Fig. S9 (a) V_{OC} , (b) FF, and (c) J_{SC} durability of 2D/3D and 3D MHP-based f-PSCs as a function of mechanical bending cycles (40% RH; ambient air; 25 °C; 4 mm minimum radius, tension-only bending).

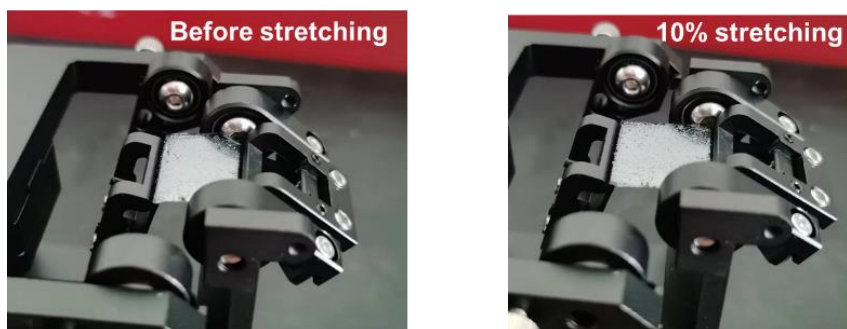


Fig. S10 Photographs of the stretching test, the sample structure is MHP/PEDOT:PSS/PDMS. (a) Before stretching; (b) ~10% stretching.

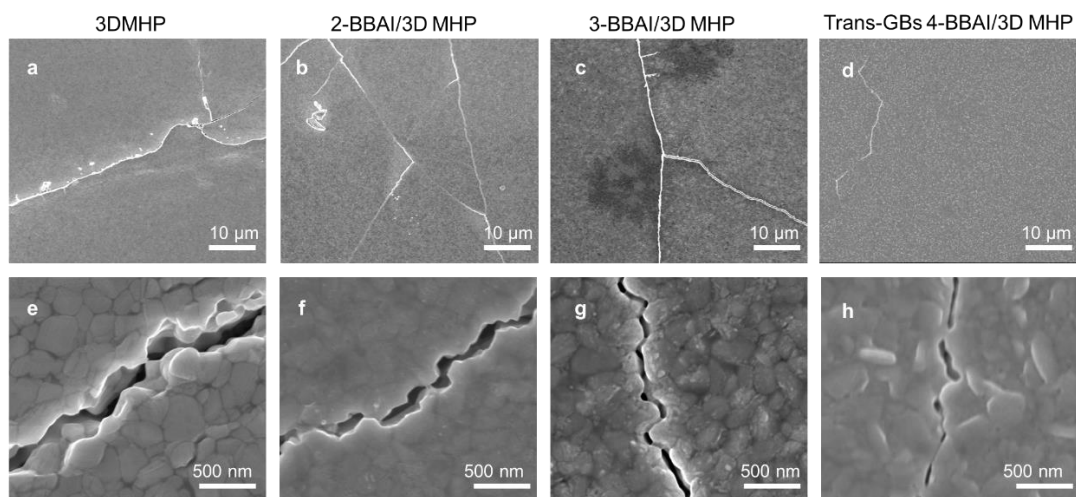


Fig. S11 Top-view SEM images of the full f-PSCs after 100-cycle stretching tests: (a, e) 3D MHP-based f-PSC; (b, f) 2-BBAI/3D MHP-based f-PSC; (c, g) 3-BBAI/3D MHP-based f-PSC; (d, h) 4-BBAI/3D MHP-based f-PSC.

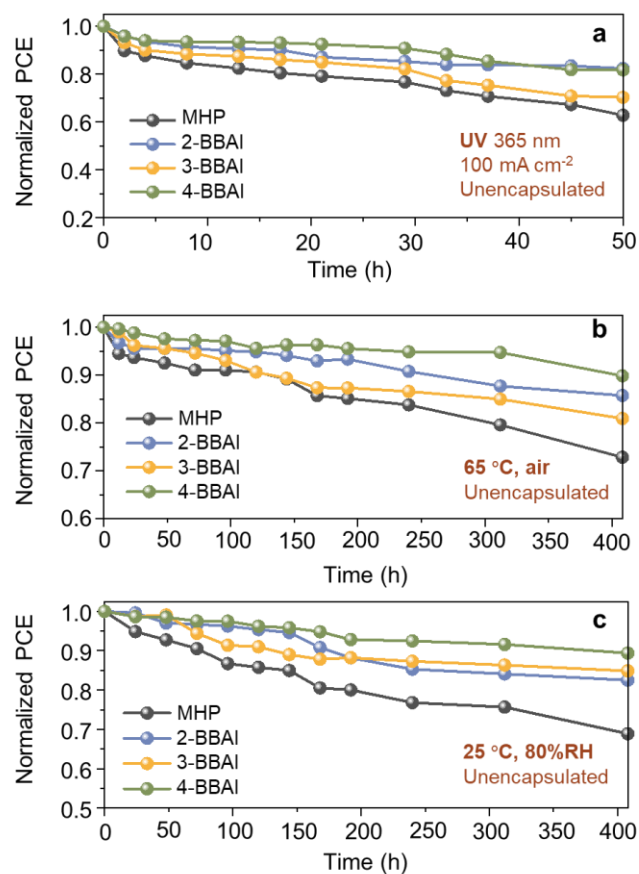


Fig. S12 PCE evolution of unencapsulated 2D/3D and 3D MHP-based f-PSCs as a function of time. (a) High-intensity UV light stability, 365 nm, 103 mW·cm⁻², 25 °C, 50% RH; (b) Thermal stability, 65 °C in the air; (c) Ambient stability, 25 °C, ~80% RH.

Table S1. PV parameters of f-PSCs with and without the 2D MHP capping layer, measured under standard AM1.5 G illumination.

Type	Scan direction		V_{OC} (V)	J_{SC} (mA mc ⁻²)	FF (%)	PCE (%)
3D	Reverse	Average	1.08 ± 0.02	22.7 ± 0.6	76.7 ± 2.7	18.8 ± 0.8
		Champion	1.09	23.1	79.6	20.0
	Forward	Average	1.05 ± 0.02	22.9 ± 0.6	74.2 ± 2.7	17.8 ± 0.8
		Champion	1.07	23.0	75.5	18.5
2-BBAI	Reverse	Average	1.13 ± 0.01	23.1 ± 0.2	80.1 ± 2.3	21 ± 0.8
		Champion	1.14	23.3	81.3	21.6
	Forward	Average	1.13 ± 0.01	23.1 ± 0.3	78.1 ± 2.7	20.3 ± 1
		Champion	1.13	23.4	79.8	21.1
3-BBAI	Reverse	Average	1.10 ± 0.01	23 ± 0.2	79.6 ± 0.9	20.1 ± 0.4
		Champion	1.10	23.4	80.0	20.7
	Forward	Average	1.06 ± 0.01	23.1 ± 0.2	77.3 ± 2	18.9 ± 0.7
		Champion	1.06	23.6	77.0	19.3
4-BBAI	Reverse	Average	1.14 ± 0.02	23.1 ± 0.3	80.4 ± 1.3	21.1 ± 0.6
		Champion	1.16	23.3	81.5	21.9
	Forward	Average	1.13 ± 0.02	23.1 ± 0.2	79.8 ± 1.2	20.8 ± 0.6
		Champion	1.15	23.3	80.1	21.5